Volcano and ship tracks indicate excessive aerosol-induced cloud water increases in a climate model

Velle Toll[1], **Matthew Christensen**[2], **Santiago Gassó**[3,4], **Nicolas Bellouin**[1]

[1]Department of Meteorology, University of Reading, Reading, UK.
[2]Atmospheric, Oceanic and Planetary Physics, University of Oxford, Oxford, UK.
[3]GESTAR, Morgan State University, Baltimore, MD, USA.
[4]Climate and Radiation Laboratory, NASA/GSFC, Greenbelt, MD, USA.

Key Points:

- Volcano and ship tracks reveal bidirectional changes in cloud water in response to aerosols, dependent on meteorological conditions
- In contrast to common behaviour of climate models, observations suggest that increases in cloud water are closely compensated by decreases
- Accounting for the aerosol enhanced entrainment would offset cloud water increases and result in weaker indirect effects in climate models

Corresponding author: Velle Toll, v.toll@reading.ac.uk

Abstract

Aerosol-cloud interaction is the most uncertain mechanism of anthropogenic radiative forcing of Earth's climate, and aerosol-induced cloud water changes are particularly poorly constrained in climate models. By combining satellite retrievals of volcano and ship tracks in stratocumulus clouds, we compile a unique observational dataset and confirm that liquid water path (LWP) responses to aerosols are bidirectional, and on average the increases in LWP are closely compensated by the decreases. Moreover, the meteorological parameters controlling the LWP responses are strikingly similar between the volcano and ship tracks. In stark contrast to observations, there are substantial unidirectional increases in LWP in the Hadley Centre climate model, because the model accounts only for the decreased precipitation efficiency and not for the enhanced entrainment drying. If the LWP increases in the model were compensated by the decreases as the observations suggest, its indirect aerosol radiative forcing in stratocumulus regions would decrease by 45%.

1 Introduction

The largest uncertainty in anthropogenic radiative forcing of Earth's climate over the industrial period is associated with aerosol-cloud interactions, and cloud water responses to aerosols are especially uncertain [*Boucher et al.*, 2013]. A larger number of aerosol particles serving as cloud condensation nuclei can increase the number of droplets in a cloud and lead to decreased droplet sizes. This process results in the enhancement of the cloud albedo - causing more reflection of shortwave radiation back to space, referred to as the first aerosol indirect or the Twomey effect [*Twomey*, 1974]. A larger number of smaller droplets can also affect cloud water due to rapid adjustments referred to as the second aerosol indirect effect. In contemporary global climate models (GCMs), it is common that the second aerosol indirect effect acts to strongly enhance the negative forcing induced by the first indirect effect [*Ghan et al.*, 2016] following the cloud lifetime hypothesis of *Albrecht* [1989], which assumes that decreased collision-coalescence efficiency of cloud droplets suppresses precipitation. In GCMs, this process is parameterised as decreased autoconversion of cloud water to rain water leading to unidirectional increases in liquid water path (LWP), although there is large diversity between different GCMs in the magnitude of the LWP increases [*Quaas et al.*, 2009; *Ghan et al.*, 2016]. Recent research suggests that the cloud water increases are not as universal as assumed in GCMs [*Stevens and Feingold*, 2009; *Malavelle et al.*, 2017], raising the question of the fidelity of the representation of second aerosol indirect effect in GCMs and highlighting the need for better observational constraints.

There is increasing evidence from global satellite observations [*Han et al.*, 2002; *Lebsock et al.*, 2008; *Chen et al.*, 2014; *Michibata et al.*, 2016] and process-level modelling [*Wang et al.*, 2003; *Ackerman et al.*, 2004; *Wood*, 2007; *Bretherton et al.*, 2007; *Xue et al.*, 2008; *Hill et al.*, 2009; *Seifert et al.*, 2015] that challenge the cloud lifetime hypothesis and suggest that LWP increases or decreases in warm clouds in response to aerosols depend on different meteorological parameters like the occurrence of rain, boundary layer stability, cloud height and relative humidity above clouds (to name the most prominent). The decreases in LWP are induced by enhanced cloud top entrainment drying in polluted clouds, which results from enhanced evaporation [*Small et al.*, 2009; *Hill et al.*, 2009] and decreased cloud droplet sedimentation [*Bretherton et al.*, 2007] caused by more numerous, smaller droplets. *Ackerman et al.* [2004] suggested, using large eddy modelling, that when cloud top entrainment is enhanced, the relative humidity above cloud has strong control over the net change in LWP.

Volcano tracks, linear cloud features formed in response to volcanic emissions beneath clouds, can be thought of as natural experiments of aerosol-cloud interactions and ship tracks as their anthropogenic analogues. The volcano and ship tracks have yet unexploited potential for constraining LWP responses in GCMs. The tracks can be detected

in marine stratocumulus clouds, which provide an excellent testbed to evaluate the upper limit of LWP increases in GCMs, where stratocumulus LWP is especially sensitive to aerosols due to the high importance of autoconversion in generating precipitation in the stratocumulus clouds [e.g. *Zhang et al.*, 2016]. Although observations of ship tracks have been used for multiple decades to improve the understanding of cloud responses to aerosols [*Coakley Jr et al.*, 1987], more extensive analysis of LWP changes in ship tracks has emerged more recently [*Christensen and Stephens*, 2011; *Chen et al.*, 2012, 2015]. These analyses have shown, similarly to process-level modelling and satellite-based studies, that LWP in polluted clouds can both increase or decrease depending on the meteorological conditions and cloud type. Regarding volcano tracks, *Gassó* [2008] published an analysis of LWP changes in just a couple of cases. More recently, *Malavelle et al.* [2017] studied monthly LWP anomalies in the area affected by a large fissure eruption in Iceland, detecting no change in LWP on average over a broad regional-scale domain. However, those studies have not identified the physical mechanisms inducing the LWP changes, and did not compare the cloud responses to ship tracks.

Here, we identify more than 900 volcano tracks and combine them with ship tracks to compile a unique observational database of aerosol-induced LWP responses. We then evaluate the realism of LWP responses in marine stratocumulus clouds in the Hadley Centre Global Environmental Model version 3 (HadGEM3). Moreover, we carry out a novel comparison between LWP responses in observations and in GCM depending on different meteorological parameters to identify the physical mechanisms responsible for the disagreements in the LWP responses. Finally, we estimate the difference in the aerosol indirect radiative forcing in stratocumulus regions in HadGEM3 that results from constraining the LWP changes based on observations of volcano and ship tracks.

2 Data and methods

2.1 Analysis of volcano and ship tracks

Cloud properties in volcano and ship tracks are compared to the nearby unpolluted cloud properties using Moderate Resolution Imaging Spectroradiometer (MODIS) collection 6 1-km resolution level 2 cloud products MYD06_L2 from Aqua and MOD06_L2 from Terra [*Platnick et al.*, 2017]. The observations of 1451 ship tracks (Figure S1 in the supporting information) originate from *Christensen and Stephens* [2012] and *Chen et al.* [2012] from various stratocumulus regions in the period 2006-2009. In addition, we identify 912 volcano tracks originating from South Sandwich Islands and Kuril Islands (Figure S1) in the period 2012-2016. The 2.1-μm near-infrared (NIR) signatures resulting from decreased cloud droplet sizes [*Coakley Jr et al.*, 1987] are used to identify volcano and ship tracks. Pixels are classed as polluted and unpolluted by sampling 2.1-μm NIR reflectance across tracks following the automated scheme for identifying ship tracks in *Segrin et al.* [2007]. Cloud properties are averaged over 20-km long and about 30-km wide segments before comparing the polluted properties to the unpolluted properties.

MODIS cloud retrievals are screened to include only pixels with single layer, low-level liquid water clouds. For ship tracks, pixels with cloud top temperature below 0 °C are excluded. For volcano tracks, pixels with infrared cloud phase being ice or mixed-phase are excluded. Although 15% of volcano tracks have solar zenith angles larger than 70° and are associated with larger retrieval uncertainties [*Grosvenor and Wood*, 2014], it does not affect the results of our paper as explained in the supporting information. The calculation of relative change in cloud droplet number concentration (CDNC) based on MODIS retrievals follows *Brenguier et al.* [2000] and *Quaas et al.* [2006] assuming that

$$CDNC \propto {R_e}^{-5/2} COD^{1/2}, \tag{1}$$

where COD is cloud optical depth and R_e is cloud droplet effective radius. Cloud albedo (A) is calculated from MODIS LWP, R_e and solar zenith angle using the BUGSrad two-

stream radiative transfer code [*Stephens et al.*, 2001]. The cloud albedo susceptibility to increases in CDNC in volcano and ship tracks is compared to susceptibility expected just from the Twomey effect assuming constant LWP [*Platnick and Twomey*, 1994; *Ackerman et al.*, 2000], which is estimated as

$$\frac{\Delta A}{A(1-A)} = \frac{\Delta ln(CDNC)}{3}. \quad (2)$$

In addition to MODIS retrievals, relative humidity from the ERA-Interim reanalysis [*Dee et al.*, 2011] is used. The analysis methods of volcano and ship tracks are detailed in the supporting information.

2.2 Model experiments

The Global Atmosphere configuration [*Walters et al.*, 2017] of the HadGEM3 GCM [*Hewitt et al.*, 2011] is used to simulate stratocumulus cloud response to doubling CDNC. Global 5-year simulations are performed at 1.25°X1.875° horizontal resolution with 85 hybrid-height vertical levels. The prognostic cloud fraction and condensation cloud scheme [*Wilson et al.*, 2008] is used with prognostic treatment of rain [*Abel and Boutle*, 2012]. Autoconversion represents the LWP response to aerosols in the GCM and the parameterization of autoconversion in HadGEM3 follows *Tripoli and Cotton* [1980]. Parameterization of mixing at the top of boundary layer follows *Lock et al.* [2000], where radiative cooling at the cloud top, evaporative cooling of entrained air, and production of turbulence through surface heating and wind shear determine the entrainment rate. The modelled grid box mean LWP response is compared with the observations as no changes in cloud fraction are detected in volcano and ship tracks based for the MODIS retrievals at 5 km spatial scale. However, changes in cloud fraction at sub-pixel resolution are possible as lidar measurements from Cloud-Aerosol Lidar and Infrared Pathfinder Satellite Observations (CALIPSO) show a marked increase in cloud fraction between polluted and unpolluted ship track segments embedded in open cell clouds [*Christensen and Stephens*, 2012]. All experiments are nudged [*Telford et al.*, 2008] towards ERA-Interim reanalysis [*Dee et al.*, 2011] above 3 km.

In the control experiment (CNTRL-EXP) monthly 3-dimensional CDNC distribution is taken from a simulation with interactive aerosols [*Mann et al.*, 2010] and an aerosol activation scheme [*West et al.*, 2014]. In two perturbation experiments, monthly CDNC is doubled in the boundary layer of stratocumulus regions (Figure S1) compared to CNTRL-EXP. FULLINDIRECT-EXP accounts for the first and second aerosol indirect effect. TWOMEY-EXP only accounts for the first indirect effect. Monthly differences between FULLINDIRECT-EXP, TWOMEY-EXP and CNTRL-EXP are analysed in the stratocumulus regions only. Model experiment design is detailed in the supporting information.

3 Results

3.1 Observations of volcano and ship tracks

Comparing polluted cloud properties within the tracks with the nearby unpolluted cloud properties reveals close similarities in cloud responses between the volcano and ship tracks. This is explained by the very similar dependencies of LWP changes on different characteristics of the atmosphere (Figure 1). In both the volcano and ship tracks, LWP tends to increase more readily in raining clouds (Figures 1 and 2). LWP tends to decrease more readily when the air above clouds is dry. In higher clouds, associated with less stable boundary layer, LWP tends to decrease more readily compared to the lower clouds (Figure 1) in agreement with *Chen et al.* [2014]. Decreased LWP in non-raining clouds with dry air above clouds and increased LWP in raining clouds in volcano and ship tracks (Figure 2) is in good agreement with *Ackerman et al.* [2004] and *Chen et al.* [2014].

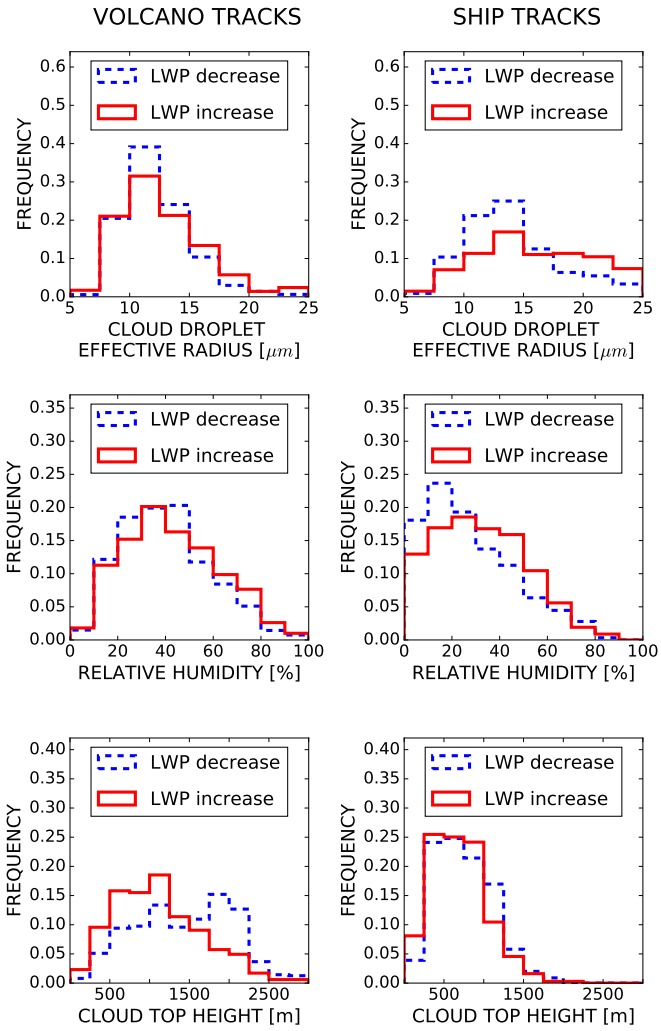

Figure 1. Frequency distributions of LWP increases and decreases in volcano and ship tracks depending on the unpolluted cloud droplet size, relative humidity above clouds and cloud top height.

Although there are substantial changes in LWP of either sign in individual tracks, the changes are small on average in both the volcano and ship datasets. On average, the LWP decreases by 1.9% in the volcano tracks and increases by 3.7% in the ship tracks (Table S1 in the supporting information). Although the average absolute LWP value is decreased in ship tracks, the average relative LWP change is positive, indicating that LWP decreases tend to occur in thicker clouds (Table S1). Moreover, the unpolluted clouds in volcano track regions are thicker compared to the ship track regions. Overall, the LWP decreases in 57% of the volcano tracks and in 55% of the ship tracks (Figure 3b). No changes in average cloud fraction are detected in the volcano or ship tracks based on the 1-km resolution MODIS retrievals used in this study. However, the cloud fraction calculated from 1-km resolution cloud masks is 100% for most of the track segments.

In both the volcano and ship tracks there are substantial decreases in cloud droplet effective radii (Table S1) and the average relative increases in cloud albedo ($\Delta A/[A(1-A)]$) are close to those expected just from the first indirect effect assuming constant LWP

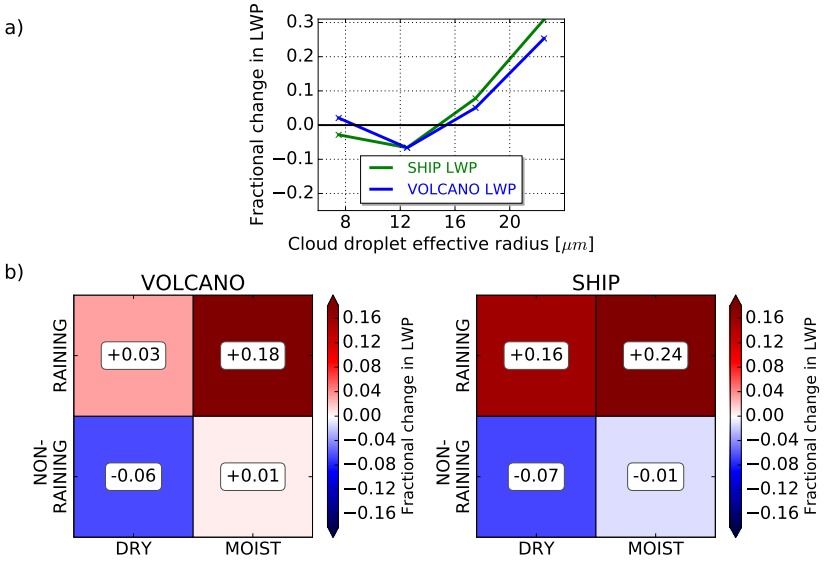

Figure 2. a) Binned fractional changes in LWP depending on cloud droplet effective radius (μm). b) Fractional change in LWP depending on occurrence of precipitation and above cloud relative humidity simultaneously. The DRY label indicates RH <= 50%, MOIST indicates RH > 50%. Clouds with cloud droplet effective radius >= 15 μm are labelled RAINING, and clouds with cloud droplet effective radius < 15 μm are labelled NON-RAINING following [*Rosenfeld et al.*, 2012]. Average values for fractional changes in LWP are given with numbers and in colour.

(Eq. 2, Figure 3a). In individual tracks, the relative change in cloud albedo is to a large extent determined by the change in LWP. The cloud albedo is decreased in 14% of the volcano tracks and 22% of the ship tracks (Figure 3b) due to strong decreases in LWP.

3.2 Model compared to observations

A clear dependence of the LWP response on cloud top height and above-cloud relative humidity is detected similarly in the volcano and ship tracks (Figures 4a and 4b). If above-cloud relative humidity is less than 30%, LWP decreases on average in both data sets. In addition, LWP tends to decrease when cloud top is higher than 1 km. In the volcano and ship tracks, there is on average an increase in LWP in lower clouds with moist air above the clouds and a decrease in LWP in higher clouds with dry air above the clouds (Figure 4b). However, cloud top height has a stronger control over the LWP responses in the volcano tracks and above-cloud relative humidity is more important in the ship tracks. The median cloud top height and above cloud relative humidity are higher in volcano tracks compared to the ship tracks (Table S1).

In HadGEM3 FULLINDIRECT-EXP, LWP is always increasing in stratocumulus regions independent of meteorological conditions (Figures 4a and 4b). The average LWP increase is 14.5%. The LWP increases in the GCM are explained by decreases in precipitation rates resulting from decreased autoconversion of cloud water to rain water (Figure 4a). The GCM does not capture the dependence of LWP response on the above-cloud relative humidity. Similarly to observations, LWP increases more in lower clouds than in higher clouds also in the GCM. However, LWP increases in all clouds in the model, irrespective of their heights. In HadGEM3 FULLINDIRECT-EXP total cloud fraction is 1.5% higher in stratocumulus regions compared to the CNTRL-EXP.

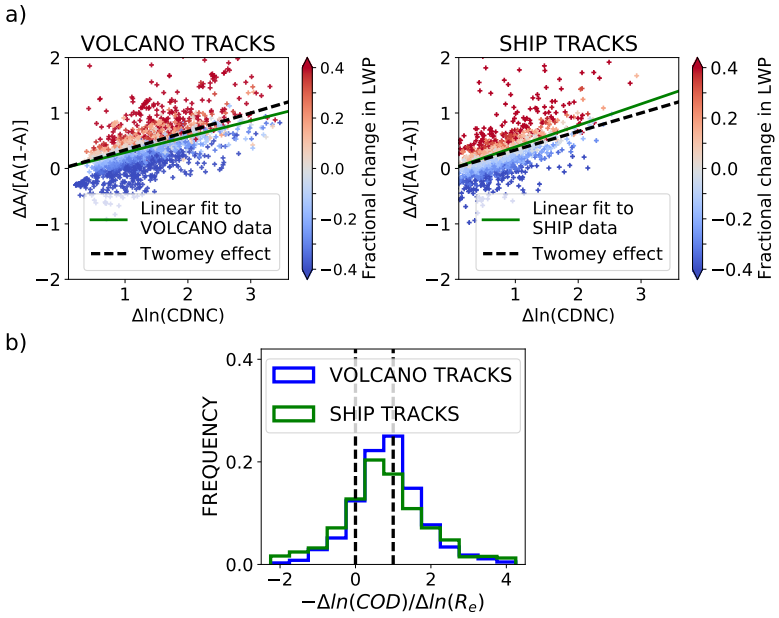

Figure 3. a) Cloud albedo susceptibility ($\Delta A/[A(1\text{-}A)]$) compared to relative change in CDNC ($\Delta ln(CDNC)$) in volcano and ship tracks. Solid green lines (forced through the origin) show least-square fits to cloud albedo susceptibility in volcano and ship tracks. The dashed black lines show the slope of 1/3 expected just from the Twomey effect assuming constant LWP. Fractional changes in LWP for individual tracks are given in colour. b) Frequency distributions comparing the changes in cloud optical depth ($-\Delta ln(COD)$) with the changes in droplet radii ($\Delta ln(R_e)$) in volcano and ship tracks. If this ratio is less (larger) than 1, then LWP is decreased (increased) in polluted clouds. If this ratio is less (larger) than 0, then cloud albedo is decreased (increased) in polluted clouds, since cloud droplet effective radii are always decreased in the polluted clouds studied.

Strong radiative forcing induced by the unidirectional LWP increases in the GCM is not in agreement with the weak second aerosol indirect effect seen on average in the volcano and ship tracks. The total indirect aerosol forcing in stratocumulus regions in response to doubling the CDNC in FULLINDIRECT-EXP compared to CNTRL-EXP is -10.7 W/m^2. The forcing in TWOMEY-EXP is only -5.9 W/m^2, which indicates, that if the LWP responses in HadGEM3 were as negligible as indicated by the observations, the aerosol indirect radiative forcing in stratocumulus regions would decrease by 45%. Perturbed marine stratocumulus clouds also lead to sizeable global forcing. When the forcing due to perturbations in the stratocumulus regions is scaled up to a global average, it is -0.10 W/m^2 in TWOMEY-EXP and -0.35 W/m^2 in FULLINDIRECT-EXP.

4 Discussion and conclusions

We compiled a unique observational dataset for constraining LWP responses to aerosols by identifying hundreds of volcano tracks in stratocumulus clouds and combining these with previously identified ship tracks. The striking similarity in cloud responses between the volcano and ship tracks suggests that the LWP responses are driven by the meteorological conditions and cloud type, rather than the way aerosols are injected into the clouds or the aerosol type. In individual volcano and ship tracks the LWP can strongly increase or decrease. The volcano and ship tracks indicate that the LWP tends to increase more readily in precipitating clouds and in lower clouds associated with more stable con-

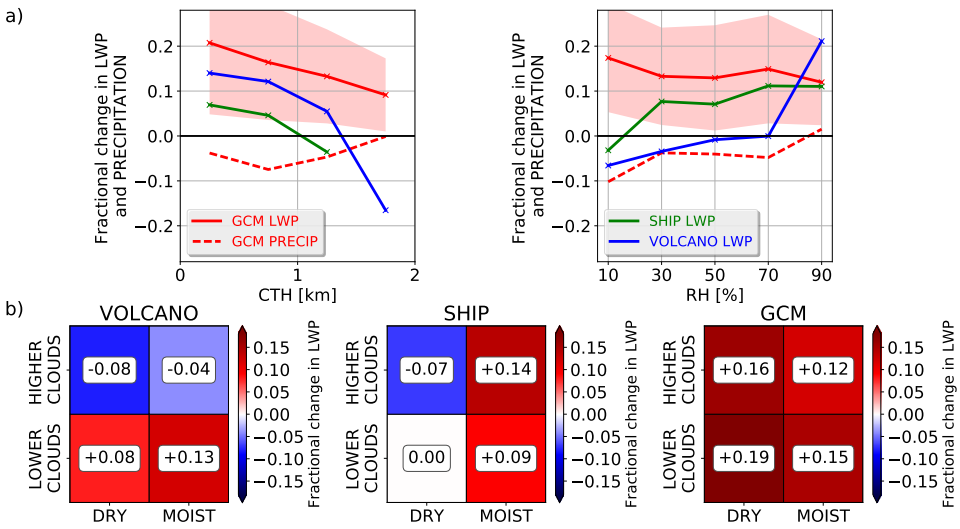

Figure 4. a) Binned fractional changes in LWP depending on cloud top height (CTH) (km) and above-cloud relative humidity (RH) (%). Bins are 500-m wide for CTH and 20% wide for RH. Fractional changes in GCM precipitation rates (GCM PRECIP) are shown with dashed red lines. Area within ±1 standard deviation of LWP changes in each bin in the GCM is shaded. b) Fractional change in LWP depending on CTH and RH simultaneously. The DRY label indicates RH <= 25%, MOIST indicates RH > 25%. Please note that these RH thresholds are different from those in Figure 2 to have equal number of observations in each bin. Clouds with CTH > 1km and CTH <= 2 km are labelled HIGHER CLOUDS, and clouds with CTH <= 1 km are labelled LOWER CLOUDS. Average values for fractional changes in LWP are given with numbers and in colour.

ditions, and that the LWP decreases are caused by the enhanced cloud top entrainment drying controlled by the relative humidity above clouds. Moreover, decreased LWP in non-raining clouds with dry air above clouds is in good agreement with high resolution modelling results of *Ackerman et al.* [2004] and an analysis of A-Train satellite observations by *Chen et al.* [2014].

On average, volcano tracks suggest a weak LWP decrease of 1.9%, and ship tracks suggest a weak LWP increase of 3.7%. Somewhat stronger LWP decreases in volcano tracks are possibly caused by the less frequent precipitation, indicated by less frequent occurrence of large droplets compared to the ship tracks, and occurrence of higher clouds (Table S1) that characterize the regions where volcanoes are located in this study. Due to slightly different data screening procedures compared with the ship tracks, the volcano tracks also potentially include some mixed phase clouds, which might contribute to stronger LWP decreases [*Christensen et al.*, 2014]. Both the volcano and ship tracks indicate that the net change in LWP and the associated radiative forcing are small, but the sign of the net LWP changes is uncertain, as it is dependent on the relative frequency of meteorological conditions favouring LWP changes of either sign. Global analysis of A-Train satellite observations by *Chen et al.* [2014] suggest that the LWP responses in marine warm clouds globally are negative under wider range of meteorological conditions than the responses in volcano and ship tracks detected in stratocumulus clouds. However, LWP responses in volcano and ship tracks are more direct observations of cloud perturbations and are not relying on a correlative analysis between aerosols and cloud properties as is *Chen et al.* [2014].

No changes in cloud fraction were detected in either volcano or ship tracks from 1-km horizontal resolution cloud masks. However, there can be changes in cloud fraction at the sub-kilometer spatial scale not studied in this work. Using CALIPSO data, *Christensen and Stephens* [2012] detected increased cloud fraction in ship tracks embedded in open cell stratocumulus clouds. Aerosol-induced transition of open cell stratocumulus clouds to closed cell clouds with higher cloud fraction is also shown by *Rosenfeld et al.* [2006] and *Goren and Rosenfeld* [2012]. *Goren and Rosenfeld* [2014] show that aerosol-induced delay in opening of the closed cells can considerably increase in-cloud LWP and cloud fraction, but such analysis of transitional cases only does not give the representative average cloud responses. *Gryspeerdt et al.* [2016] propose that the linkage between aerosol distribution and cloud fraction is largely explained by meteorological covariations, but if requiring CDNC to mediate the relationship between aerosol optical depth and cloud fraction, higher cloud fraction is still observed when more aerosol is present. Further research on volcano and ship tracks using sub-kilometer scale data could help to separate aerosol influence on the total cloud water amount into in-cloud LWP and cloud fraction changes.

We compare cloud water responses to aerosols in volcano and ship tracks with the perturbations in large scale cloud sheets. Expecting similar LWP response for local and larger scale perturbations is justified by large eddy modelling of ship tracks [*Berner et al.*, 2015] and large eddy modelling of stratus/stratocumulus clouds [*Ackerman et al.*, 2004; *Bretherton et al.*, 2007], showing that LWP increases result from suppressed precipitation and LWP decreases result from enhanced entrainment in polluted clouds. However, changes in mesoscale circulation across the volcano and ship tracks cannot be entirely excluded, and further work is needed to determine the overall importance of the modified local scale circulation.

In stark contrast to the observations, there are substantial unidirectional increases in LWP in stratocumulus regions in HadGEM3 in response to doubling CDNC, with the average LWP increase being 14.5%. LWP increases result from suppressed precipitation as the rate of autoconversion decreases with increasing CDNC. The entrainment parameterization in the GCM [*Lock et al.*, 2000] does not explicitly include aerosol impact on cloud-top entrainment through decreased cloud droplet sedimentation [*Bretherton et al.*, 2007] and/or enhanced cloud droplet evaporation [*Small et al.*, 2009; *Hill et al.*, 2009], probably resulting in the inability to simulate LWP decreases in the GCM. This inability reveals itself as an insensitivity of the LWP response to relative humidity above clouds.

One potential solution to improve the representation of LWP responses could be to avoid parameterizing LWP responses to aerosol changes because the net response is likely to be weak as suggested by the volcano and ship tracks. In order to capture the more nuanced behaviour and the spatio-temporal variability of the LWP responses that depend on meteorological conditions, multi-variate probability density functions-based parameterizations [*Guo et al.*, 2011] could be used as they reproduce bidirectional LWP responses. Using the observations of volcano and ship tracks together with high resolution modelling provides a great opportunity for further development of GCMs to improve the representation of cloud water response to aerosols, especially for representing both LWP decreases and increases in response to aerosol perturbations. Specifically, these observations together with high resolution models could help to further evaluate entrainment parameterizations in GCMs.

Volcano and ship tracks provide unequivocal evidence for the excessive LWP increases in contemporary GCMs. In addition, they provide support for the weaker satellite-based estimates of the LWP responses to aerosols [*Quaas et al.*, 2009; *Michibata et al.*, 2016], and the less negative inverse estimates of aerosol radiative forcing [*Murphy et al.*, 2009; *Stevens*, 2015] compared to the estimates based on GCMs. In HadGEM3, neglecting second indirect effect leads to a 45% decrease in total aerosol indirect forcing in stratocumulus regions. Yet, HadGEM3's LWP increases in response to aerosol changes are weak compared to other GCMs [*Ghan et al.*, 2016; *Malavelle et al.*, 2017]. In those mod-

els, observational constraints from volcano and ship tracks would most probably lead to even larger weakening of aerosol indirect forcing. Such a substantial weakening of the aerosol radiative forcing in climate models would ultimately translate into reduced uncertainties in projections of the future climate.

Acknowledgments

This study is funded by the University of Reading, with support from the CLouds and Aerosol Radiative Impacts and Forcing: Year 2016 (CLARIFY-2016) project, funded by the UK Natural Environment Research Council under grant agreement NE/L013479/1. The MODIS cloud products MYD06_L2 from Aqua and MOD06_L2 from Terra used in this study were obtained from Atmosphere Archive & Distribution System (LAADS) Distributed Active Archive Center (DAAC), located in the Goddard Space Flight Center in Greenbelt, Maryland (https://ladsweb.nascom.nasa.gov/). ERA-Interim data was obtained from ECMWF archive using ECMWF Web-API.

References

Abel, S., and I. Boutle (2012), An improved representation of the raindrop size distribution for single-moment microphysics schemes, *Quarterly Journal of the Royal Meteorological Society*, *138*(669), 2151–2162.

Ackerman, A. S., O. B. Toon, J. P. Taylor, D. W. Johnson, P. V. Hobbs, and R. J. Ferek (2000), Effects of aerosols on cloud albedo: Evaluation of Twomey's parameterization of cloud susceptibility using measurements of ship tracks, *Journal of the Atmospheric Sciences*, *57*(16), 2684–2695.

Ackerman, A. S., M. P. Kirkpatrick, D. E. Stevens, and O. B. Toon (2004), The impact of humidity above stratiform clouds on indirect aerosol climate forcing, *Nature*, *432*(7020), 1014.

Albrecht, B. A. (1989), Aerosols, cloud microphysics, and fractional cloudiness, *Science*, *245*(4923), 1227–1231.

Berner, A., C. Bretherton, and R. Wood (2015), Large eddy simulation of ship tracks in the collapsed marine boundary layer: a case study from the Monterey area ship track experiment, *Atmospheric Chemistry and Physics*, *15*(10), 5851.

Boucher, O., D. Randall, P. Artaxo, C. Bretherton, G. Feingold, P. Forster, V.-M. Kerminen, Y. Kondo, H. Liao, U. Lohmann, et al. (2013), Clouds and aerosols, in *Climate change 2013: the physical science basis. Contribution of Working Group I to the Fifth Assessment Report of the Intergovernmental Panel on Climate Change*, pp. 571–657, Cambridge University Press.

Brenguier, J.-L., H. Pawlowska, L. Schüller, R. Preusker, J. Fischer, and Y. Fouquart (2000), Radiative properties of boundary layer clouds: Droplet effective radius versus number concentration, *Journal of the atmospheric sciences*, *57*(6), 803–821.

Bretherton, C., P. N. Blossey, and J. Uchida (2007), Cloud droplet sedimentation, entrainment efficiency, and subtropical stratocumulus albedo, *Geophysical research letters*, *34*(3).

Chen, Y.-C., M. Christensen, L. Xue, A. Sorooshian, G. Stephens, R. Rasmussen, and J. Seinfeld (2012), Occurrence of lower cloud albedo in ship tracks, *Atmospheric Chemistry and Physics*, *12*(17), 8223–8235.

Chen, Y.-C., M. W. Christensen, G. L. Stephens, and J. H. Seinfeld (2014), Satellite-based estimate of global aerosol-cloud radiative forcing by marine warm clouds, *Nature Geoscience*, *7*(9), 643.

Chen, Y.-C., M. W. Christensen, D. J. Diner, and M. J. Garay (2015), Aerosol-cloud interactions in ship tracks using Terra MODIS/MISR, *Journal of Geophysical Research: Atmospheres*, *120*(7), 2819–2833.

Christensen, M., K. Suzuki, B. Zambri, and G. Stephens (2014), Ship track observations of a reduced shortwave aerosol indirect effect in mixed-phase clouds, *Geophysical Research Letters*, *41*(19), 6970–6977.

Christensen, M. W., and G. L. Stephens (2011), Microphysical and macrophysical responses of marine stratocumulus polluted by underlying ships: Evidence of cloud deepening, *Journal of Geophysical Research: Atmospheres*, *116*(D3).

Christensen, M. W., and G. L. Stephens (2012), Microphysical and macrophysical responses of marine stratocumulus polluted by underlying ships: 2. Impacts of haze on precipitating clouds, *Journal of Geophysical Research: Atmospheres*, *117*(D11).

Coakley Jr, J. A., R. L. Bernstein, and P. A. Durkee (1987), Effect of ship-stack effluents on cloud reflectivity, *Science*, *237*, 1020–1023.

Dee, D., S. Uppala, A. Simmons, P. Berrisford, P. Poli, S. Kobayashi, U. Andrae, M. Balmaseda, G. Balsamo, P. Bauer, et al. (2011), The ERA-Interim reanalysis: Configuration and performance of the data assimilation system, *Quarterly Journal of the royal meteorological society*, *137*(656), 553–597.

Gassó, S. (2008), Satellite observations of the impact of weak volcanic activity on marine clouds, *Journal of Geophysical Research: Atmospheres*, *113*(D14).

Ghan, S., M. Wang, S. Zhang, S. Ferrachat, A. Gettelman, J. Griesfeller, Z. Kipling, U. Lohmann, H. Morrison, D. Neubauer, et al. (2016), Challenges in constraining anthropogenic aerosol effects on cloud radiative forcing using present-day spatiotemporal variability, *Proceedings of the National Academy of Sciences*, *113*(21), 5804–5811.

Goren, T., and D. Rosenfeld (2012), Satellite observations of ship emission induced transitions from broken to closed cell marine stratocumulus over large areas, *Journal of Geophysical Research: Atmospheres*, *117*(D17).

Goren, T., and D. Rosenfeld (2014), Decomposing aerosol cloud radiative effects into cloud cover, liquid water path and Twomey components in marine stratocumulus, *Atmospheric research*, *138*, 378–393.

Grosvenor, D., and R. Wood (2014), The effect of solar zenith angle on MODIS cloud optical and microphysical retrievals within marine liquid water clouds, *Atmospheric Chemistry and Physics*, *14*(14), 7291–7321.

Gryspeerdt, E., J. Quaas, and N. Bellouin (2016), Constraining the aerosol influence on cloud fraction, *Journal of Geophysical Research: Atmospheres*, *121*(7), 3566–3583.

Guo, H., J.-C. Golaz, and L. Donner (2011), Aerosol effects on stratocumulus water paths in a PDF-based parameterization, *Geophysical Research Letters*, *38*(17).

Han, Q., W. B. Rossow, J. Zeng, and R. Welch (2002), Three different behaviors of liquid water path of water clouds in aerosol–cloud interactions, *Journal of the atmospheric sciences*, *59*(3), 726–735.

Hewitt, H., D. Copsey, I. Culverwell, C. Harris, R. Hill, A. Keen, A. McLaren, and E. Hunke (2011), Design and implementation of the infrastructure of HadGEM3: The next-generation Met Office climate modelling system, *Geoscientific Model Development*, *4*(2), 223–253.

Hill, A. A., G. Feingold, and H. Jiang (2009), The influence of entrainment and mixing assumption on aerosol–cloud interactions in marine stratocumulus, *Journal of the Atmospheric Sciences*, *66*(5), 1450–1464.

Lebsock, M. D., G. L. Stephens, and C. Kummerow (2008), Multisensor satellite observations of aerosol effects on warm clouds, *Journal of Geophysical Research: Atmospheres*, *113*(D15).

Lock, A., A. Brown, M. Bush, G. Martin, and R. Smith (2000), A new boundary layer mixing scheme. Part I: Scheme description and single-column model tests, *Monthly weather review*, *128*(9), 3187–3199.

Malavelle, F. F., J. M. Haywood, A. Jones, A. Gettelman, L. Clarisse, S. Bauduin, R. P. Allan, I. H. H. Karset, J. E. Kristjánsson, L. Oreopoulos, et al. (2017), Strong constraints on aerosol–cloud interactions from volcanic eruptions, *Nature*, *546*(7659), 485–491.

Mann, G., K. Carslaw, D. Spracklen, D. Ridley, P. Manktelow, M. Chipperfield, S. Pickering, and C. Johnson (2010), Description and evaluation of GLOMAP-mode: A modal global aerosol microphysics model for the UKCA composition-climate model, *Geoscientific Model Development*, *3*(2), 519–551.

Michibata, T., K. Suzuki, Y. Sato, and T. Takemura (2016), The source of discrepancies in aerosol–cloud–precipitation interactions between GCM and A-Train retrievals, *Atmospheric Chemistry and Physics*, *16*(23), 15,413–15,424.

Murphy, D., S. Solomon, R. Portmann, K. Rosenlof, P. Forster, and T. Wong (2009), An observationally based energy balance for the Earth since 1950, *Journal of Geophysical Research: Atmospheres*, *114*(D17).

Platnick, S., and S. Twomey (1994), Determining the susceptibility of cloud albedo to changes in droplet concentration with the Advanced Very High Resolution Radiometer, *Journal of Applied Meteorology*, *33*(3), 334–347.

Platnick, S., K. G. Meyer, M. D. King, G. Wind, N. Amarasinghe, B. Marchant, G. T. Arnold, Z. Zhang, P. A. Hubanks, R. E. Holz, et al. (2017), The MODIS cloud optical and microphysical products: Collection 6 updates and examples from Terra and Aqua, *IEEE Transactions on Geoscience and Remote Sensing*, *55*(1), 502–525.

Quaas, J., O. Boucher, and U. Lohmann (2006), Constraining the total aerosol indirect effect in the LMDZ and ECHAM4 GCMs using MODIS satellite data, *Atmospheric Chemistry and Physics*, *6*(4), 947–955.

Quaas, J., Y. Ming, S. Menon, T. Takemura, M. Wang, J. E. Penner, A. Gettelman, U. Lohmann, N. Bellouin, O. Boucher, et al. (2009), Aerosol indirect effects–general circulation model intercomparison and evaluation with satellite data, *Atmospheric Chemistry and Physics*, *9*(22), 8697–8717.

Rosenfeld, D., Y. Kaufman, and I. Koren (2006), Switching cloud cover and dynamical regimes from open to closed Benard cells in response to the suppression of precipitation by aerosols, *Atmospheric Chemistry and Physics*, *6*(9), 2503–2511.

Rosenfeld, D., H. Wang, and P. J. Rasch (2012), The roles of cloud drop effective radius and lwp in determining rain properties in marine stratocumulus, *Geophysical Research Letters*, *39*(13).

Segrin, M. S., J. A. Coakley Jr, and W. R. Tahnk (2007), MODIS observations of ship tracks in summertime stratus off the west coast of the United States, *Journal of the Atmospheric Sciences*, *64*(12), 4330–4345.

Seifert, A., T. Heus, R. Pincus, and B. Stevens (2015), Large-eddy simulation of the transient and near-equilibrium behavior of precipitating shallow convection, *Journal of Advances in Modeling Earth Systems*, *7*(4), 1918–1937.

Small, J. D., P. Y. Chuang, G. Feingold, and H. Jiang (2009), Can aerosol decrease cloud lifetime?, *Geophysical Research Letters*, *36*(16).

Stephens, G. L., P. M. Gabriel, and P. T. Partain (2001), Parameterization of atmospheric radiative transfer. Part I: Validity of simple models, *Journal of the atmospheric sciences*, *58*(22), 3391–3409.

Stevens, B. (2015), Rethinking the lower bound on aerosol radiative forcing, *Journal of Climate*, *28*(12), 4794–4819.

Stevens, B., and G. Feingold (2009), Untangling aerosol effects on clouds and precipitation in a buffered system, *Nature*, *461*(7264), 607.

Telford, P., P. Braesicke, O. Morgenstern, and J. Pyle (2008), Description and assessment of a nudged version of the new dynamics Unified Model, *Atmospheric Chemistry and Physics*, *8*(6), 1701–1712.

Tripoli, G. J., and W. R. Cotton (1980), A numerical investigation of several factors contributing to the observed variable intensity of deep convection over south Florida, *Journal of Applied Meteorology*, *19*(9), 1037–1063.

Twomey, S. (1974), Pollution and the planetary albedo, *Atmospheric Environment (1967)*, *8*(12), 1251–1256.

Walters, D., I. Boutle, M. Brooks, M. Thomas, R. Stratton, S. Vosper, H. Wells, K. Williams, N. Wood, T. Allen, et al. (2017), The Met Office unified model global atmosphere 6.0/6.1 and JULES global land 6.0/6.1 configurations, *Geoscientific Model Development*, *10*(4), 1487.

Wang, S., Q. Wang, and G. Feingold (2003), Turbulence, condensation, and liquid water transport in numerically simulated nonprecipitating stratocumulus clouds, *Journal of the atmospheric sciences*, *60*(2), 262–278.

West, R., P. Stier, A. Jones, C. Johnson, G. Mann, N. Bellouin, D. Partridge, and Z. Kipling (2014), The importance of vertical velocity variability for estimates of the indirect aerosol effects, *Atmospheric Chemistry and Physics*, *14*(12), 6369–6393.

Wilson, D. R., A. C. Bushell, A. M. Kerr-Munslow, J. D. Price, and C. J. Morcrette (2008), PC2: A prognostic cloud fraction and condensation scheme. I: Scheme description, *Quarterly Journal of the Royal Meteorological Society*, *134*(637), 2093–2107.

Wood, R. (2007), Cancellation of aerosol indirect effects in marine stratocumulus through cloud thinning, *Journal of the atmospheric sciences*, *64*(7), 2657–2669.

Xue, H., G. Feingold, and B. Stevens (2008), Aerosol effects on clouds, precipitation, and the organization of shallow cumulus convection, *Journal of the Atmospheric Sciences*, *65*(2), 392–406.

Zhang, S., M. Wang, S. J. Ghan, A. Ding, H. Wang, K. Zhang, D. Neubauer, U. Lohmann, S. Ferrachat, T. Takeamura, et al. (2016), On the characteristics of aerosol indirect effect based on dynamic regimes in global climate models, *Atmospheric Chemistry and Physics*, *16*(5), 2765–2783.